ARTICLE

Inorganic salts and Organic matter effects on nanorod, nanowire, and nanoplate MoO_3 aggregation, dissolution, and photocatalysis

Received 00th January 20xx,
Accepted 00th January 20xx

DOI: 10.1039/x0xx00000x

Sofia K. Fanourakis, [a] Janire Peña-Bahamonde, [b] and Debora F. Rodrigues [† a,b]

Use of visible light photocatalytic nanomaterials in water treatment can be promising in treating contaminants. However, little research has been conducted examining the effects of more complex chemistries in the nanomaterial's performance. In this work, the effects of inorganic salts (NaCl and $CaCl_2$) and natural organic matter (NOM) such as humic acid (HA) and extracellular polymeric substances (EPS) on nanoparticle aggregation, dissolution, and ultimately on the photocatalytic properties of molybdenum trioxide (MoO_3), *i.e.* nanorods, nanowires, and nanoplates were examined. In the presence of NaCl, nanorod, nanowire, and nanoplate MoO_3 had similar critical coagulation concentrations, while the nanorods showed higher instability in $CaCl_2$. Overall, the presence of inorganic salts caused high colloidal instability in the MoO_3 nanostructures in terms of aggregation behavior, but greatly aided in the reduction of MoO_3 dissolution. NOM presence decreased aggregation rates, albeit dissolution was not similarly affected in all three structures. Only the dissolution of the nanowire structures was reduced in the presence of HA or EPS. Furthermore, the photocatalytic activity of the nanowires and nanoplates was overall reduced when inorganic salts or natural organic matter were present. While the presence of natural organic matter alone did reduce photocatalytic effectiveness of the nanorod MoO_3, the presence of salts seemed to negate the effects from the organic compounds. Furthermore, the presence of $CaCl_2$ resulted in a highly enhanced photocatalytic activity regardless of the presence of natural organic matter. The structural and chemical differences of the nanomaterials played a significant role in their aggregation, dissolution, and ability to photocatalytically degrade methylene blue in solution. This study demonstrates that a better understanding of water chemistry effects on nanomaterials is essential prior to their intended applications.

Keywords: Molybdenum trioxide, nanorods, nanowires, nanoplates, photocatalytic activity, aggregation, natural organic matter

Introduction

Engineered nanomaterials have attracted great research interest due to their unique properties that differ from the properties of the bulk material. For instance, nanosized MoO_3 has been shown to have a variety of uses owing to its photocatalytic, capacitive, gas sensing, optical, and oxidative properties.[1–7] MoO_3 has been of particular interest in water treatment due to its ability to be used in a great variety of applications and ability to control its shape and size.[8,9] The chemical and electrical properties of the nanomaterial can be altered by controlling the size and shape of the material. For example, MoO_3 structure can be controlled by altering synthesis parameters such as amount and type of reagents present (i.e. amount and type of acid, absence or presence and type of surfactant), and different crystal structures can be synthesized, such as h- or α- MoO_3.[1,10] The different MoO_3 morphologies have been shown to have different chemical and electrical properties, which can affect their dissolution and photocatalytic properties in different solution chemistries.[1] Despite many studies showing MoO_3 can be promising in water treatment, it has recently been shown that its high solubility can lessen its utility.[1] However, no systematic studies have been performed thus far examining the stability (aggregation behaviour and dissolution) and photocatalytic activity of different morphologies of MoO_3 in complex water chemistry solutions containing inorganic salts and/or natural organic matter (NOM).

Numerous studies have been conducted on other nanomaterials such as TiO_2, ZnO, SiO_2, CeO_2, and Ag examining how inorganic salts and NOM – specifically, humic acid (HA) – affect nanoparticle stability in solution.[2,11–19] Highly stable material in solution present with low solubility and minimal to no aggregation. Aggregation in particular can be an important measure of nanoparticle colloidal stability, which is greatly influenced by the presence of inorganic and organic compounds.[20] For example, the presence of inorganic salts can cause nanoparticle aggregation and presence of organic matter can stabilize nanoparticles significantly.[20,21] However,

[a] Department of Materials Science and Engineering, University of Houston, Houston, TX 77204 – 4003.
[b] Department of Civil and Environmental Engineering, University of Houston, Houston, TX 77204 – 4003.

† Corresponding Author: Debora F. Rodrigues, email: dfrigirodrigues@uh.edu

depending on the stabilization mechanism (steric hindrance or surface modification), the properties of the material may be altered.[1,18,22,23] For instance, peroxymonosulfate degradation of methylene blue can be either positively or negatively affected by the presence of HA depending on whether the concentration of HA is low or high, respectively.[24] TiO_2 photocatalytic activity is hindered by the presence of HAs since these organic material can compete for active sites on the photocatalyst or act as light screens.[23] Furthermore, increased aggregation can also hinder photocatalytic activity by reducing the available surface area effectively reducing light absorption.[23] Thus, the presence of inorganic salts can greatly hinder photocatalyst degradative properties.

Solution chemistry is an important factor to consider when examining the photocatalytic properties of a material. However, nanomaterial photocatalytic activity is understudied in complex solutions. In this study, the photocatalytic degradation of methylene blue (MB) was examined in the presence of inorganic salts (NaCl or $CaCl_2$) and NOM such as HA or extracellular polymeric substances (EPS) produced by *E. coli*. These organic and inorganic compounds can be present in waters undergoing water treatment; thus, it is important to understand their effect on the nanomaterials' properties. Therefore, to understand the effect of organic and inorganic compounds on the degradative properties of structurally different MoO_3 nanomaterials, not only was their ability to degrade MB investigated in complex solutions, but the aggregation kinetics and dissolution properties of the nanomaterials were also examined.

Experimental

Materials

The chemicals used were purchased and utilized as received from Sigma Aldrich and include: Ammonium molybdate tetrahydrate ($(NH_4)_6Mo_7O_{24} \cdot 4H_2O$), sodium chloride (NaCl), calcium chloride ($CaCl_2$), Suwannee River Humic Acid (HA), sodium hydroxide (NaOH), hydrochloric acid (HCl), nitric acid (HNO_3), methylene blue (MB), potassium hydrogen phthalate, and ethanol. The hydrogen peroxide (H_2O_2 30%) was purchased from Macron Fine Chemicals.

Nanoparticle Synthesis and Characterization

All three nanoparticles were synthesized as described in our previous work.[1] Briefly, the nanorods were synthesized via the hydrothermal method in which 2.46 g of Ammonium molybdate tetrahydrate was dissolved in 20 mL MilliQ water, then 5 mL concentrated HNO_3 was added drop wise, and the solution was heated to 90 °C for 3 hours in a Teflon lined autoclave. The particles were cleaned by centrifugation using 70% ethanol and dried at room temperature. The batches of nanorods, nanowires, and nanoplates utilized were the same as our previous publication.[1] Briefly, for the nanoplates, 192 mg of molybdenum powder was added to a Teflon vessel (45 ml) containing 24 ml of ethanol under magnetic stirring. Then, 3 ml of H_2O_2 was added, and the mixture was stirred for 0.5 h to obtain a yellow solution. The Teflon vessel was then sealed in a stainless-steel autoclave, heated, and maintained at 160 °C for 14 h. The product was collected by centrifugation (Thermo Scientific Sorvall Legend XTR Centrifuge), washed with ethanol and dried under vacuum. The nanowires were prepared using the same procedure as the nanoplates with the difference of using 384 mg of molybdenum powder, 30 ml of isopropanol, and 5 ml of H_2O_2.

The characterization was done by using scanning electron microscopy (SEM) (Nova NanoSEM 230) to examine the morphology of the crystal samples. Samples were first coated with gold for 30 seconds (Denton Desk V) and then examined with the SEM at accelerating voltage equal to 5 kV at different magnifications (15000x for the nanorods, 30000x for the nanowires, and 40000x for the nanoplates). Crystallographic information of samples was obtained via X-ray diffraction (XRD) using Rigaku MiniFlex 600 diffractometer with a Cu anode (40 kV and 15 mA) at a scanning rate of 0.05° per second from 5° to 80° in 2θ. These materials were extensively characterized (XPS, FTIR, and bandgap measurements) in our previous publication.[1]

Stock Solution Preparation

For each of the three nanomaterials, 1000 ppm stock solutions were prepared by mixing 3 mg of each nanoparticle in 3 mL MilliQ water and sonicating for 15 min in a bath sonicator (Branson 1800) to create more evenly dispersed particle solutions. Stock solutions were utilized within three hours to ensure dissolution was kept to a minimum (less than 20%).

A stock solution of 1 M NaCl was prepared by dissolving 1.23 g of NaCl in 100 mL MilliQ water. Similarly, to prepare a stock solution of 100 mM $CaCl_2$, 1.4 g $CaCl_2$ were dissolved in 100 mL MilliQ water. For the preparation of the stock HA solution, 50 mg of HA were dispersed into 50 mL MilliQ water. The total organic carbon (TOC) of this solution was measured and determined to be 13.16 ppm using the TOC Analyzer instrument (Shimadzu, TOC-L CPH) and using known concentrations of potassium hydrogen phthalate (1, 5, 10, 50, and 100 ppm) for the calibration curve.

To prepare a stock solution of EPS, *E. coli* K12 was grown in M63 media[25] at 25°C for 48 hours until the culture was turbid at which point the cultures were centrifuged and filtered through a 0.2 μm vacuum filtration system to eliminate any cells present in solution. Then, they were combined and transferred to a dialysis bag (Spectrum labs 54 mm regenerated cellulose dialysis membrane with a 3.5 kDa pore size), which was kept in MilliQ water. The first day the MilliQ water was exchanged three times every three hours. Then the water was exchanged twice a day until the conductivity of the water matched that of the MilliQ water to ensure any salts from the media were removed and the salt content could be controlled for the experiments. Similar to the HA, the TOC of the EPS was determined using the TOC Analyzer instrument, which determined the EPS stock solution to have a TOC of 2.16 ppm.

All stock solutions (nanomaterial, NaCl, $CaCl_2$, HA, and EPS) did not have their pH adjusted for the experiments performed at pH 5, but had their pH adjusted to 7 for the experiments performed at pH 7 using 0.1 M NaOH.

Particle ζ-potential

Particle charge in solution was measured using the ZetaSizer (Malvern Nano ZS, Malvern) instrument and using the zeta potential transfer standard DTS 1235. Stock solutions of each nanoparticle were diluted from 1000 ppm to 250 ppm and approximately 1 mL of the diluted solution of each nanoparticle was transferred to a folded capillary cell for measurement. The concentration of 250 ppm of the nanoparticles was determined to be an appropriate concentration for acquiring stable measurements with minimal error. Measurements were collected at pH 5 and 7 and pH adjustments were performed using 1M NaOH or 1M HCl. Measurements were performed in triplicate.

Particle Aggregation Behavior

The aggregation behavior of each nanoparticle was studied in different concentrations of NaCl (ranging from 1 mM to 200 mM) and different concentrations of $CaCl_2$ (ranging from 1 mM to 20 mM) using Dynamic Light Scattering (DLS) (Malvern Nano ZS, Malvern). Additionally, experiments were performed at either pH 5 or 7 in which case the pH was adjusted using 1 M NaOH. To measure aggregation kinetics of each particle, 0.375 mL stock solution was transferred to a polystyrene cuvette suitable for DLS measurements to reach a final concentration of 250 ppm for each nanoparticle. To achieve each concentration of either NaCl or $CaCl_2$, appropriate amounts of each stock solution were calculated. Then MilliQ water was added to the sample, such that once the NaCl or $CaCl_2$ was added, the total volume reached 1 mL. Next, the salt solution was added, and the cuvette was vortexed for approximately 2 seconds and immediately placed in the ZetaSizer for measurement. The ZetaSizer was set to collect 3 measurements every 3 seconds for up to 20 minutes. Measurements were performed in triplicate. The aggregation rate, r, was calculated for each measurement period using Eq. 1 [19,26,27] and subsequently Eq. 2 [19,26,27] was utilized to calculate the attachment efficiency, α. In Eq. 1, D_h denotes the hydrodynamic diameter measured by the DLS instrument and N_0 is the initial concentration of the nanoparticles. In Eq. 2, r denotes the aggregation rate at a particular concentration and $r_{diffusion\ limited}$ is the aggregation rate at which the aggregation rate is no longer influenced by a change in ionic strength (IS).

$$r \propto \frac{1}{N_0}\left(\frac{d\,D_h(t)}{dt}\right)_{t\to 0} \quad (1)$$

$$\alpha = \frac{r}{r_{diffusion\ limited}} \quad (2)$$

The effect of humic acid on the aggregation behavior of each nanomaterial was studied to determine the minimum required concentration for colloidal stabilization of the nanoparticles. First, 0.5 ppm TOC of humic acid was studied at pH 5 and 7. Because there were minimal differences between aggregation rates between both pH values, the concentration of humic acid was increased to 1 ppm TOC and studied at pH 7. Finally, the effect of 1 ppm TOC of EPS was determined at pH 7. To achieve this condition, 0.75 mL of the stock EPS solution was added to the cuvette. These experiments were performed at the following conditions: 30 mM NaCl, 200 mM NaCl, 3 mM $CaCl_2$, and 15 mM $CaCl_2$. These conditions were selected such that for each type of salt the aggregation behavior would be either reaction or diffusion limited. Measurements were performed in triplicate.

Particle Dissolution – Effects of salts and NOM

The solubility of each nanoparticle was examined in 6 mL MilliQ water at pH 7 with the concentration of each nanoparticle starting at 250 ppm. The dissolution of each material was quantified using Atomic Absorption Spectroscopy (AAS) (AAnalyst 200, Perkin Elmer) equipped with a Molybdenum lamp from Perkin Elmer and using duplicate samples and triplicate measurements per sample. The following solution conditions were examined: 200 mM NaCl, 15 mM $CaCl_2$, 1 ppm HA, and 1 ppm EPS. To achieve each condition, appropriate amounts from the stock solutions were added in MilliQ water and the nanoparticles were introduced, the solutions were mixed, and left standing for 3 hours at room temperature (~25 °C). A time length of three hours was chosen based on our previous work in which all three nanomaterial were able to significantly degrade MB by three hours.[1] However, in that work the nanowire MoO_3 was much faster in removing MB, thus lower concentrations of nanomaterial and MB were analyzed in this work to allow for an improved comparison of the properties of each material in the presence of a variety of chemical conditions. Finally, the solutions were filtered using centrifugal Amicon ultrafiltration tubes (30,000 NMWL). The recovered solution was diluted 1:5 in order to ensure the measurements were within the linear range of the instrument.

Methylene Blue Decolorization

Photocatalytic experiments were performed at pH 7 to measure the change in coloration of methylene blue (MB) in aqueous suspensions of MoO_3 under different chemical conditions. The chemical conditions tested included the presence of the following solution conditions and combinations of solutions: a) 200 mM NaCl, b) 15 mM $CaCl_2$, c) 1 ppm HA, d) 1 ppm EPS, e) 200 mM NaCl and 1 ppm HA, f) 200 mM NaCl and 1 ppm EPS, g) 15 mM $CaCl_2$ and 1 ppm HA, and h) 15 mM $CaCl_2$ and 1 ppm EPS. Samples were exposed to visible light (Nexlux LED light, which utilizes the 5050 RGB LED package with a wavelength range of 400 to 700 nm and maximum luminous intensities of 100, 400, and 100 mcd for the red, green, and blue regions, respectively). The lights were mounted on the inside of a cylindrical hard surface to be able to provide even lighting when on a magnetic plate stirrer (Heidolph). The samples were first arranged circularly on a shallow glass container with the diameter of the stirring plate such that each would receive an equal amount of light. Then, they were placed on the stirrer plate and the lights

were mounted on the plate. A small amount of water was placed in the glass container and its temperature was controlled to room temperature using a water pumping system. The initial concentration of MB was fixed at 25 mg/L with a catalyst loading of 250 mg/L and a final volume of 6 mL. Prior to photooxidation, the solution was stirred in the dark for 30 min to establish an adsorption–desorption equilibrium.[1] After 3 hours of irradiation 0.5 mL of each sample solution was removed and centrifuged (Thermo Scientific Sorvall Legend XTR Centrifuge) at 12,000 rpm for 5 min to separate photocatalysts from the mixture. MB absorbance was measured using a UV–Vis spectrometer, SynergyMX Microtiter plate reader (Biotek) at λ = 664 nm. The experiments were performed in triplicate and the results were analyzed and reported as coloration of MB. The data for the MB coloration when nanoparticles were present were adjusted to remove the effects of any complexation occurring between MB and the ions and NOM present in the solutions.

Statistical Analysis of Results

The aggregation, dissolution, and MB degradation data (acquired by methods described in sections 2.4-2.7) were analyzed using the GraphPad Prism 8 software. A two-way ANOVA test was utilized along with Tukey's multiple comparison test to determine statistical significance of the results.

Results and Discussion

Characterization

SEM images (Figure 1) of the material and XRD (Figure 2) for the nanorods, nanowires, and nanoplates show the material utilized in this study, which is the same batch also used and thoroughly characterized in our previous publication.[1] New SEM images and XRD data were acquired showing that the morphologies shown in Figure 1 and crystallographic information depicted in Figure 2 match our previously published data.[1]

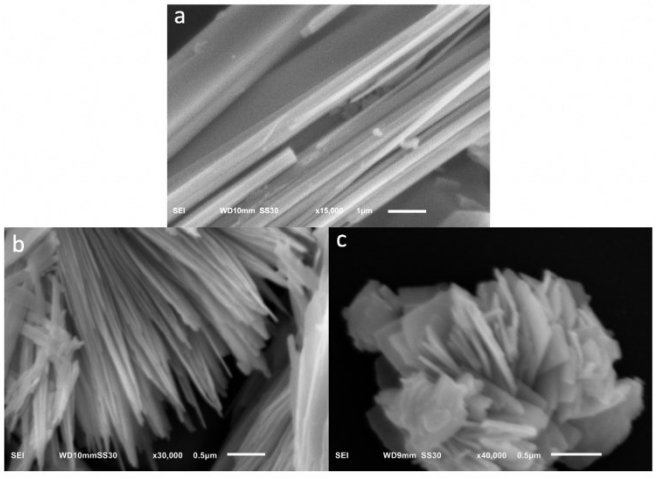

Figure 1: SEM images of a) nanorods (×15,000 magnification), b) nanowires (×30,000 magnification), and c) nanoplates (×40,000 magnification).

The nanowires and nanorods presented diameters in the range of 59 nm and 180 nm, respectively, with lengths greater than 5 μm. The nanoplates had a thickness around 74 nm and a width of approximately 180 nm. The XRD patterns for the three nanomaterials showed strong diffraction peaks indicating a highly crystalline morphology. Furthermore, the nanoplate and nanowire XRD peaks were indexed as orthorhombic MoO_3 (JCPDS – 35-0569), while for the nanorods they were indexed as hexagonal (JCPDS – 21-0569).

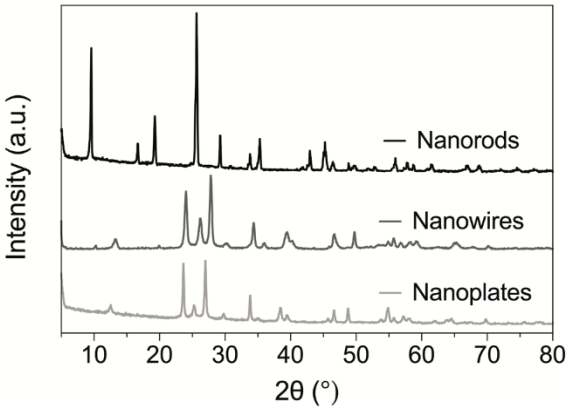

Figure 2: XRD of each MoO_3 nanomaterial from 5° to 80° (2θ)

Effects of pH and NOM in nanoparticle charge and aggregation kinetics

The ζ-potential of each particle was measured at pH 5 and 7 (Figure 3) to provide information on the charge of the particles in solution. The nanorods and nanowires showed a decrease in potential (more negative) as pH increased from 5 to 7.

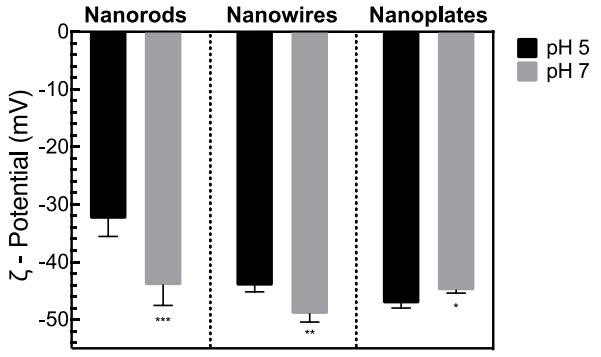

Figure 3: ζ-potentials of each nanomaterial at pH 5 and 7 in MilliQ water at room temperature (25°C). Stars indicate statistical significance between the pH 5 and 7 results for each nanoparticle. Stars indicate statistical significance between the pH 5 and 7 results for each nanoparticle (one star indicates $p<0.05$, two stars indicate $p<0.005$, and three stars indicate $p<0.0001$).

These more negative results are expected since an increase in pH can cause the deprotonation of surface OH groups. This decrease in potential could also be caused by the breakdown of the crystal structure due to increased dissolution at higher pH values (the increased presence of hydroxyl ions facilitates MoO_3 dissolution and, thus, molybdate ion formation).[1,28,29] The

nanoplates showed an increase in potential with the change in pH (the nanoplate surface in pH 7 became more positively charged). The different nanostructures exhibit differences in their Mo^{+6}:Mo^{+5} ratio (20.3, 6.4, and 0.5 for nanorods, nanowires, and nanoplates, respectively), which relates to the dissolution of the nanostructures, where nanorods dissolve more than nanowires and nanoplates.[1] Unlike the nanorods and nanowires, the nanoplates did not dissolve as much (only around 20% at basic pH after 6 days), and they contained an increased ratio of Mo^{+5} to Mo^{+6} in their structure, which was caused by oxygen vacancies in the MoO_3 structure.[1] Such vacancies can be filled by hydroxyl groups.[30] Thus, it is likely that the introduction of OH^- ions interacts with the Mo^{+5} structures, filling oxygen vacancies, decreasing the concentration of hydroxyl ions in solution, thus, preventing the deprotonation of surface -OH groups and making the particles' surface charge slightly less negative with this slight increase in pH.

The ζ- potential of each particle was further examined in the presence of either increasing concentrations of NaCl or $CaCl_2$ (Figure 4). As expected, with increasing IS, there was an increase in the ζ-potential of the material (the material becomes less negatively charged). At higher ionic strengths, the change in ζ-potential became less and less negatively charged since the electrical double layer becomes more and more compressed with the increase of IS.[27] Additionally, the presence of $CaCl_2$ affected the surface charge more significantly than NaCl and much smaller changes in potential were observed. This is expected as the adsorption of calcium ions (a divalent ion) on the surface of the material increases the positive charges on the surface much more than sodium ions (a monovalent ion), thus, surface neutralization is greater with the presence of calcium ions rather than sodium ions.[27,31,32] Furthermore, since the size of the two cations is similar, the differences that were observed indicate that charge is the most important factor, while cation size does not play a role in this case. Similar to these results, a greater effect from $CaCl_2$ than NaCl has also been observed when investigating ZnO aggregation.[31] Interestingly, as the IS of NaCl is increased from 30 mM to 60 mM, the change in potential became larger for the nanorods and nanowires than the nanoplates This may indicate that the presence of more Mo^{6+} than Mo^{5+}, which also contributes to the elongated structure of the nanorods and nanowires, influences the electrical double layer compression as IS changes. Furthermore, the ζ-potentials each reach a plateau value indicating that they have reached a maximum compression of the electrical double layer and the charge of the material is no longer affected by the increasing ionic strength.[32]

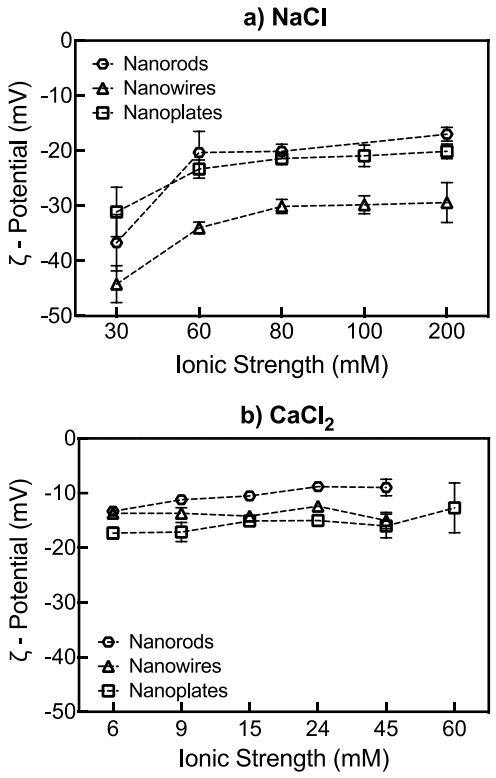

Figure 4: ζ- potential of each nanomaterial (nanorods, nanowires, nanoplates) in (a) NaCl and (b) $CaCl_2$ salt solutions in MilliQ water adjusted to pH 7 using NaOH at room temperature. Error bars correspond to the standard deviation in the measurements. The dotted lines do not represent continuity of the data; rather, they were included to aid in the viewing of the data

The attachment efficiency at each IS for each nanoparticle and for each salt (NaCl or $CaCl_2$) and pH value (5 and 7) was calculated by equation 2 and is shown in Figure 5. From these curves it is evident that the aggregation of the nanoparticles follows the reaction and diffusion limited scheme. At low IS the aggregation rate is limited by the amount of ions present in solution (referred to as the reaction limited region), and after a critical point (the critical coagulation concentration, or CCC) the aggregation rate goes from reaction limited to diffusion limited in which an increase in IS no longer affects the aggregation rate. The CCC can be used to compare the stability of nanoparticles in aqueous environments since lower CCC values indicate lower stability due to those particles being more likely to aggregate.

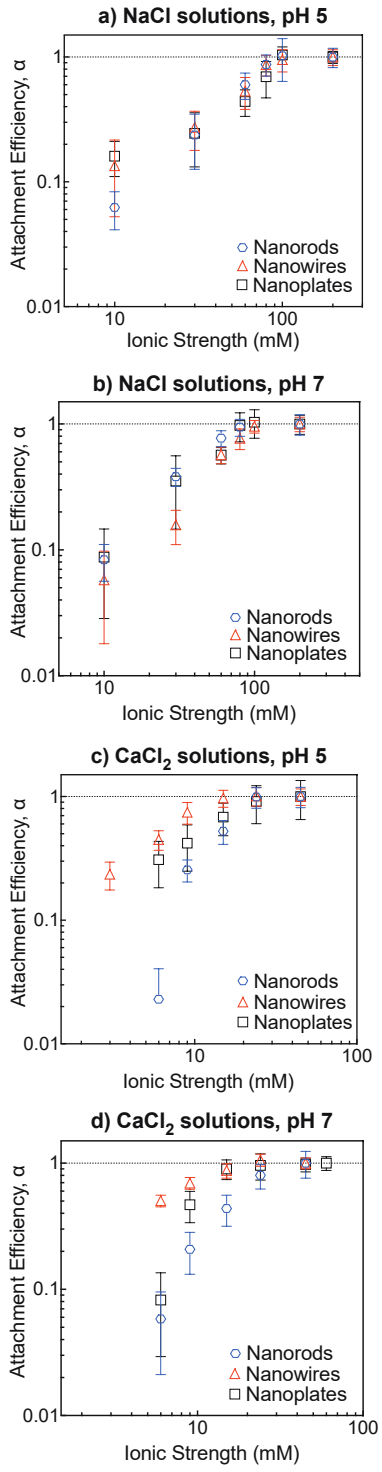

Figure 5: Attachment efficiency of each nanomaterial (nanorod, nanowire, and nanoplate) in pH 5 or 7 with increasing IS of either NaCl (10-200 mM) or $CaCl_2$ (3-45 mM).

Using the attachment efficiency curves, the critical coagulation concentrations (CCC) of each nanoparticle for each salt and pH were calculated by finding the intersection of the line describing the reaction limited region and the line describing the diffusion limited region. Based on the calculated CCCs at each pH for each nanostructure (Figure 6), all investigated particles presented similar stability at the two pH values. With NaCl present, all nanoparticles had similar stability, however, differences between the stability of the nanoparticles in the presence of $CaCl_2$ were larger than when in the presence of NaCl. In $CaCl_2$ the nanowires appear to be more stable at pH 5 than the nanorods and nanoplates. At pH 7, the nanowires and nanoplates have similar stability and the nanorods are more unstable than the nanowires and nanoplates. In addition, the nanorods have a statistically significant increase in CCC from pH 5 to 7 in the presence of $CaCl_2$ but not in the presence of NaCl. This lowering in stability at higher pH values is expected as the particles are more soluble as pH increases as presented in a previous work.[1] Furthermore, the greater change in colloidal stability when $CaCl_2$ is present rather than NaCl can be also attributed to Ca^{2+} ions contributing to a larger charge neutralization than Na^{+} ions along with potential complexation reactions and bridging effects. The nanowires followed the same pattern as the nanorods although the differences did not show statistical significance. Unlike the nanorods and nanowires, the nanoplates showed the opposite pattern; an increase in stability was seen when pH was increased from 5 to 7 (albeit the result was statistically significant only for $CaCl_2$). The difference in pattern between the materials' stabilities could be explained by the ζ-potential changes seen in Figure 3. While the nanorods and nanowires showed a higher negative potential at pH 7 than pH 5, the nanoplates show a more positive potential. Thus, an increase in pH can stabilize the nanoplates (reduce the CCC) rather than destabilize them further as with the nanorods and nanoplates (indicated by an increase in the CCC). These results complement the results from the ζ-potential measurements, further indicating that the ratio of Mo^{6+} to Mo^{5+} in the MoO_3 structure may play an important role in particle aggregation stability when salts are present and when pH is altered.

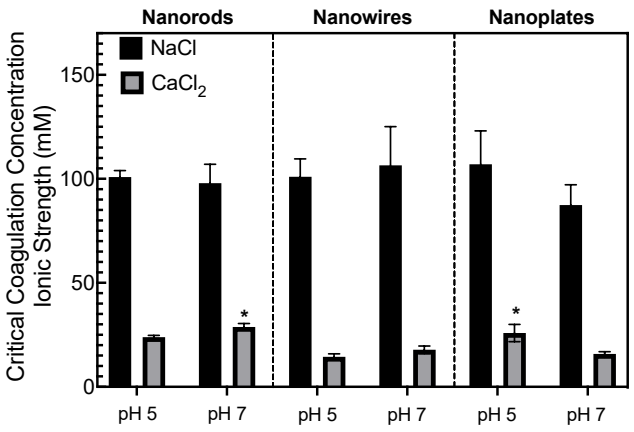

Figure 6: Critical Coagulation Concentrations (CCCs) of each nanomaterial at pH 5 and pH 7. The asterisks indicate statistically significant values when comparing the pH 5 and pH 6 CCCs for each nanoparticle and type of salt (either NaCl or $CaCl_2$).

The effect of pH and natural organic matter (HA or EPS) on the aggregation rates in the reaction and diffusion limited regions of the nanoparticle kinetics was examined using NaCl or $CaCl_2$ (Figure 7). The change in pH does not significantly affect the aggregation rate of the nanorods and nanoplates but more so

affects the aggregation rate of the nanowires when no NOMs are present and even more so when $CaCl_2$ is present instead of NaCl. This could be caused by the increased dissolution resulting from the higher pH, which would compete with the increased hydrodynamic radius caused by the aggregation of the nanoparticles due to the presence of salts (Figure 7). With the presence of 0.5 ppm TOC HA, the aggregation rates in some conditions for all three materials were reduced. These conditions include: 200 mM NaCl and 45 mM (IS) $CaCl_2$ for the nanorods, 45 mM (IS) $CaCl_2$ for the nanowires, and 200 mM NaCl, 9 mM and 45 mM (IS) $CaCl_2$ for the nanoplates. This indicates that HA at a concentration of 0.5 ppm TOC not only starts to alter the electrostatic interactions between particles, but it also starts to introduce some steric effects and may potentially adsorb to the nanoparticles reducing the aggregation rates. Since the changes in aggregation rates were not significant in any of the conditions for each nanoparticle, the TOC of HA was increased to 1 ppm. Furthermore, since for all material there was not a significant difference between the aggregation rates when 0.5 ppm HA was present and the pH was changed from 5 to 7, the pH was adjusted to 7 for the remaining experiments to provide environmentally relevant data. With a 1 ppm TOC of HA at pH 7 there was a significant reduction in aggregation rates for all conditions for the three nanomaterials. This reduction was similar when EPS was introduced instead of HA. The steric effect of NOM and the resulting stabilization of nanomaterial has been observed in a number of different studies and confirmed via theoretical calculations and observations.[18,22] These effects can have significant impact on the dissolution of the material and the ability of the photocatalyst to degrade contaminants as is discussed in the following sections.

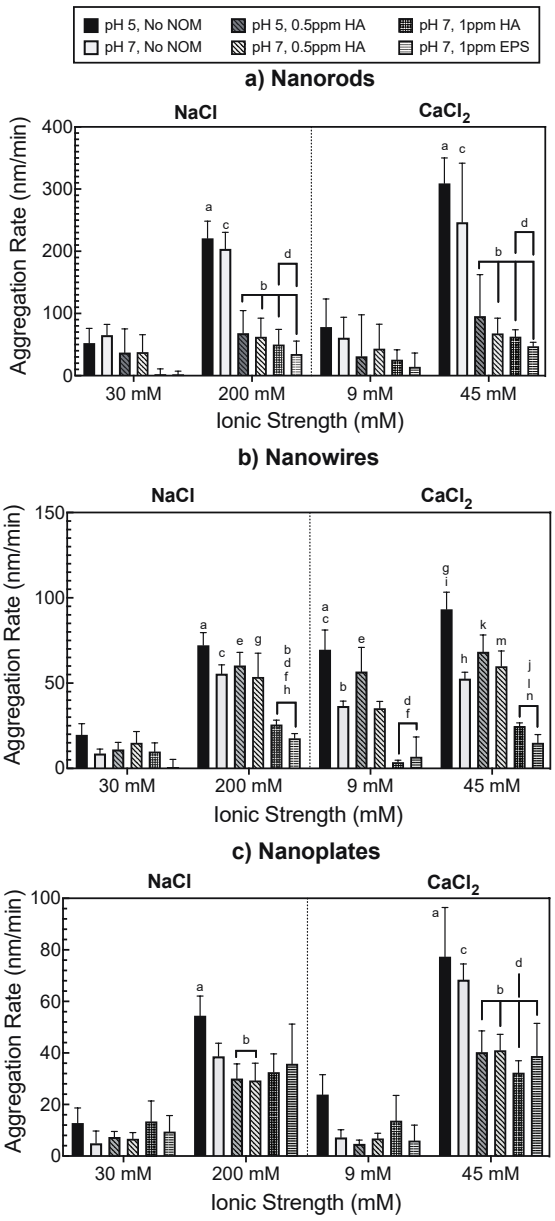

Figure 7: Effect of pH and natural organic matter (humic acid (HA), and extracellular polymeric substances (EPS)) on a) nanorod, b) nanowire, and c) nanoplate aggregation rates in the reaction limited and diffusion limited regions with NaCl or $CaCl_2$. The letters on top of each bar indicate significance when compared to the bar with the subsequent letter. For instance, the result with letter a is significantly different from the result with letter b and the result with letter c is significantly different from that with letter d. Brackets were used to group different comparisons and increase the graph's readability.

Particle Dissolution in Different Salt and Organic Matter Solutions

Nanoparticle dissolution can be affected not only by nanoparticle size and shape, but by the chemical conditions of the solution as well.[33,34] As such, the effect of salt (at a concentration at which the aggregation was diffusion limited for each salt according to the aggregation kinetics data), HA, and EPS on the dissolution of each MoO_3 structure were investigated (Figure 8). A length of time of three hours was selected for the dissolution of the nanoparticles based on the degradation results of our previous work. [1]

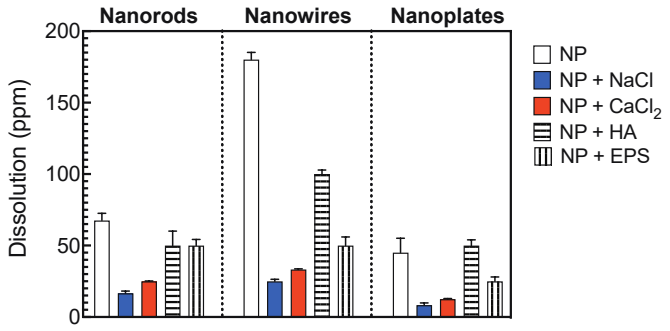

Figure 8: Dissolution of nanorods, nanowires, and nanoplate particles in different solution conditions: MilliQ water (denoted as NP in the legend), 200 mM NaCl (NP+NaCl), 15 mM (45 mM IS) $CaCl_2$ (NP+$CaCl_2$), 1 ppm HA (NP+HA), or 1 ppm EPS (NP+EPS). All solutions were adjusted to pH 7 and contained 250 ppm of the respective nanoparticle.

After 3 hours in pH 7 solution, the nanoplates are the least soluble, followed by the nanorods, and nanowires. All three material are least soluble when salts are present. The presence of salt promotes nanoparticle aggregation, which can effectively reduce the available surface area interacting with water molecules. Thus, particle dissolution can be reduced via the addition of salts.[26] Interestingly, the monovalent salt stabilizes all three particles more than the divalent salt. The IS of the monovalent salt (200 mM) was much higher than that of the divalent salt (45 mM) indicating that IS plays a more significant role in the reduction of dissolution of the nanoparticles than the valency of the cations. It has been found that metal oxide dissolution occurs due to hydroxide ion interaction with the nanomaterial surface.[35] While the presence of calcium ions provides greater surface neutralization and formation of a more compact electrostatic double layer as discussed earlier, the higher ionic strength seems to play a greater role in dissolution reduction. The increased number of cations present can be more effective in preventing hydroxyl ion interaction with the material by attaching to the negatively charged surface of the nanomaterial. In addition, the higher number of chloride ions present due to the larger IS in the case of 200 mM NaCl can provide greater steric protection thus reducing the interaction of the nanoparticles with hydroxyl ions, effectively reducing the dissolution of the nanomaterial more than when 45 mM (IS) $CaCl_2$ is present.

Furthermore, EPS reduces dissolution more than HA indicating increased interaction between the nanomaterial and EPS compared to HA. Although EPS is overall negatively charged, it contains positive and negatively charged species unlike HA, which is mainly negatively charged. Thus, the greater decrease in dissolution by EPS rather than HA is expected. The greatest reduction in solubility is seen in the nanowires, which are significantly stabilized by both salts and NOMs. Unlike the nanowires, no significant reduction in solubility is observed for the nanorods or nanoplates in the presence of HA. Likely, the structure of the nanowires plays a role in the effectiveness of the steric protection by NOM. Although the nanowires have a similar chemical makeup as the nanorods, their smaller size could potentially lead to an increase in steric protection by NOM.

The Effects of Salts and NOM on the Nanomaterial Photocatalytic Activity

Methylene blue was utilized as a model contaminant to assess the photocatalytic activity of each nanomaterial with and without the presence of salts (either 200 mM NaCl or 45 mM IS $CaCl_2$) and/or 1 ppm NOM (HA or EPS). The different conditions were tested in the dark (includes effects from adsorption and complexation) and in the light (includes effects from photocatalysis, adsorption, and complexation), and the remaining coloration of MB in solution was assessed for each condition.

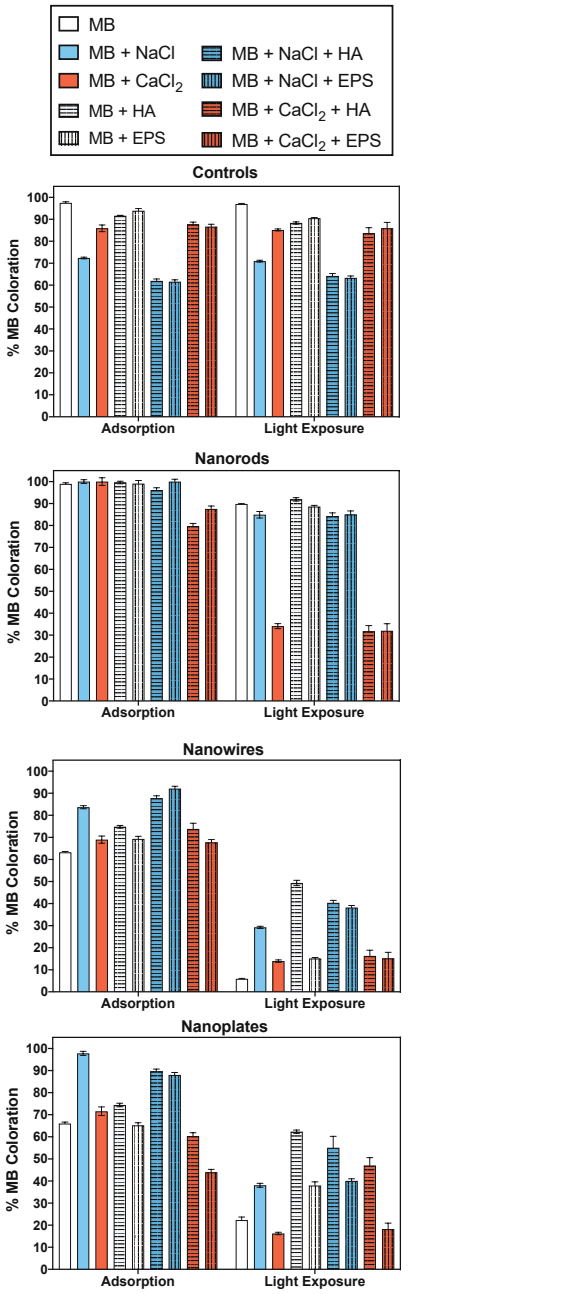

Figure 9: Effects of 200 mM NaCl, 45 mM (IS) $CaCl_2$, 1 ppm HA, and 1 ppm EPS on the removal of MB by nanorods, nanowires, and nanosheets. The effect of complexation of MB with each salt or NOM and their combinations has been removed from the nanomaterial interaction with MB.

In Figure 9, it is evident from the control experiments, which contain no nanoparticles, that some complexation occurs between MB and each salt, NOM and, combinations of salts and NOM. Additionally, without the presence of nanomaterial, no photocatalytic activity occurred. The removal of MB by NaCl was larger likely due to the higher number of Cl^- ions present from the difference of IS between NaCl and $CaCl_2$. Furthermore, the removal was higher with HA present rather than EPS, which is expected, as the ζ-potential of the HA solution was more negative than that of the EPS solution, making HA more prone to complexation with the positively charged MB. When either salt was present with either HA or EPS, the removal of MB was more prominent in the presence of the salts rather than NOM.

The effects from MB complexation with salts and/or NOM in Figure 9 (nanorods, nanowires, and nanoplates) were removed by adding the MB decolorization amount from the dark and light controls to the nanoparticle MB coloration data in the light and dark, respectively, to more accurately assess the effect of solution chemistry on nanostructure degradative properties. The type of MoO_3 present affected the removal of MB differently. For instance, the nanorods showed increased adsorption of MB when NaCl and HA, or $CaCl_2$ and HA or EPS were present. Furthermore, there was an increase in MB removal in light when each salt was present regardless of the presence of NOM. Except in the instance when NaCl and HA were present, where the increased removal in light could be accounted by the increased adsorption of MB by the material under the dark conditions. However, when $CaCl_2$ was present the photocatalytic removal of MB was greatly enhanced, and the presence of NOM did not alter the removal of MB in light. This phenomenon has been observed with other materials, however, the exact mechanism that causes increased photocatalytic activity of the nanomaterial in the presence of $CaCl_2$ has not been explored.[35] It is speculated that, in the case of carbamazepine degradation by BiOCl the presence of Ca^{2+} increases adsorption via bridging effects, thus increasing photocatalytic degradation.[35] Furthermore, it is interesting that the addition of NOM, while capable of reducing aggregation rates of the nanomaterial, does not affect MB removal. It is possible that the bridging or complexation effects due to the calcium ion have a higher affinity towards MB and the nanorods rather than the NOM present thus any NOM in the solution will not compete in the photocatalytic reaction process.

Unlike the nanorods, the nanowires and nanoplates showed a general reduction in photocatalytic activity in the presence of salt or NOM. The nanowire removal of MB was most affected by the presence of salts and NOM. The adsorption of MB was significantly reduced by each salt and NOM. This was expected as the presence of salt causes increased aggregation, thus less surface area is available for MB to adsorb to and less surface area is available for light to interact with the material.[23] In addition, with NOM present, especially with HA, the photocatalytic activity of the nanowires was greatly reduced. Likely, the increased interaction between NOM and the nanowires that results in decreased solubility also affects the ability of the material to degrade MB. This competitive interaction between MB, NOM, and the photocatalyst has also been observed in the degradation of MB by peroxymonosulfate[24] and by cobalt-doped $BiVO_4$[36].

Similar to the nanowires, the nanoplates also showed a decrease in MB adsorption but only in the presence of NaCl, $CaCl_2$, or HA. The adsorption of MB did not appear to be affected by the presence of EPS. In addition, MB adsorption was increased when both $CaCl_2$ and NOM were in the presence of nanorods. It is possible that when both $CaCl_2$ and NOM are present there is increased complexation between the nanomaterial, NOM, and MB allowing for greater adsorption of MB. For the nanoplates, however, when taking into account the increased adsorption in the presence of $CaCl_2$ and NOM, the photocatalytic activity of the material was reduced by the presence of salts or NOM.

While in our previous work we had determined that these materials would ultimately not be effective for use in water treatment due to their high solubility and low photocatalytic activity[1], taking into consideration these additional results, their usability for water treatment can be reconsidered. As per our previous work[1], for all the three different nanoparticles, we saw similar patterns where the holes are responsible for the oxidation of H_2O molecules forming hydroxyl radical and further increasing the H_2O_2 concentration. All three material showed a dramatic decrease in solubility in the presence of salts and either an enhancement or slight hindrance in photocatalytic activity. The nanorods for instance could be promising in water treatment when calcium chloride is present as it can greatly enhance the material's photocatalytic properties regardless of the NOMs present. The nanowires and nanoplates, however, do not show the same usability since their photocatalytic activity was reduced in the presence of salts and NOM. Ultimately, the importance of testing the behavior of new nanomaterial in a variety of solution chemistries is vital in understanding their usability outside the laboratory.

Conclusions

In this study the effects of inorganic salts (NaCl and $CaCl_2$) and natural organic matter (HA and EPS) on MoO_3 nanorods, nanowires, and nanoplates aggregation, dissolution, and ultimately on their photocatalytic properties of MB were examined. MoO_3 nanoparticles have shown high instability in solution due to their tendency to aggregate and dissolve. While nanorod, nanowire, and nanoplate MoO_3 had similar CCCs in NaCl, the nanorods showed higher instability in $CaCl_2$. However, all three nanomaterials showed exceptional reduction in dissolution in the presence of high ionic strength NaCl or $CaCl_2$ most likely due to the reduction in surface area caused by the

high aggregation of the material. In addition, the presence of natural organic matter, whether HA or EPS, was effective in reducing aggregation rates of the material. Furthermore, only the dissolution of the nanowire structures showed significant reduction in the presence of HA or EPS likely due to the structure and significantly smaller size of the nanowires. Overall, the presence of inorganic salts causes high colloidal instability in the MoO_3 nanostructures in terms of aggregation behavior, but greatly aids in the reduction of dissolved MoO_3. NOM presence, however, can decrease aggregation rates, albeit dissolution is not similarly affected in all three structures.

When examining the potential usability of these nanostructures for photocatalysis, the effect of inorganic and organic components can be significant. For instance, while the nanowires were significantly more stable in the presence of salts and NOM, the photocatalytic activity of the material was reduced. The nanoplates also showed a reduction in photocatalytic activity. For these nanoparticles the steric effects from the NOM seemed to play a greater role in reducing the activity of the material. For the nanorods, while the presence of NOM alone did reduce degradative effectiveness, the presence of salts seemed to negate the effects from the NOM. Furthermore, the presence of $CaCl_2$ resulted in a highly enhanced photocatalytic activity regardless of the presence of NOM. Additional experiments will be required to ascertain the exact mechanisms of photocatalytic activity enhancement by the presence of calcium chloride.

Even though all three materials were composed of MoO_3, the structural and chemical differences of the nanostructures played a significant role in their aggregation, dissolution, and ability to photocatalytically degrade MB in solution while in the presence of inorganic and organic material. This denotes the importance of thoroughly investigating new materials for their intended application. While nanorod MoO_3 may not have high utility in water treatment due to its high solubility, in the presence of $CaCl_2$, it can be a promising material in degrading water contaminants. Without testing photocatalytic materials in more complex solutions, it cannot be known how effective they can be in degrading contaminants outside of the laboratory settings.

Conflicts of interest

There are no conflicts to declare.

Acknowledgements

This work was supported by the NSF BEINM Grant Number: 1705511 and the Robert A. Welch Foundation award number (E-2011-20190330). We would like to acknowledge Dr. Jiming Bao's group, especially Dr. Chunzheng Wu, for synthesizing and providing the nanowire and nanoplate MoO_3, as well as Aprameya Sudharsan for assisting in the project. The findings achieved herein are solely the responsibility of the authors.

Notes and references

1 J. Peña-Bahamonde, C. Wu, S. K. Fanourakis, S. M. Louie, J. Bao and D. F. Rodrigues, *J. Catal.*, 2020, **381**, 508–519.
2 D. Zhou and A. A. Keller, *Water Res.*, 2010, **44**, 2948–2956.
3 D. Van Pham, R. A. Patil, C. C. Yang, W. C. Yeh, Y. Liou and Y. R. Ma, *Nano Energy*, 2018, **47**, 105–114.
4 S. S. Mahajan, S. H. Mujawar, P. S. Shinde, A. I. Inamdar and P. S. Patil, *Concentration Dependent Structural, Optical and Electrochromic Properties of MoO 3 Thin Films*, 2008, vol. 3.
5 C. S. Hsu, C. C. Chan, H. T. Huang, C. H. Peng and W. C. Hsu, *Thin Solid Films*, 2008, **516**, 4839–4844.
6 S. S. Sunu, E. Prabhu, V. Jayaraman, K. I. Gnanasekar, T. K. Seshagiri and T. Gnanasekaran, *Sensors Actuators, B Chem.*, 2004, **101**, 161–174.
7 E. Comini, L. Yubao, Y. Brando and G. Sberveglieri, *Chem. Phys. Lett.*, 2005, **407**, 368–371.
8 A. Chithambararaj, N. Rajeswari Yogamalar and A. C. Bose, *Cryst. Growth Des.*, 2016, **16**, 1984–1995.
9 A. Chithambararaj and A. C. Bose, *J. Alloys Compd.*, 2011, **509**, 8105–8110.
10 C. Chaves-Lopez, H. N. Nguyen, R. C. Oliveira, E. T. Nadres, A. Paparella and D. F. Rodrigues, *Nanoscale*, 2018, **10**, 20702–20716.
11 M. A. Schlautman and J. J. Morgan, *Geochim. Cosmochim. Acta*, 1994, **58**, 4293–4303.
12 K. Afshinnia, M. Sikder, B. Cai and M. Baalousha, *J. Colloid Interface Sci.*, 2017, **487**, 192–200.
13 A. Kroll, R. Behra, R. Kaegi and L. Sigg, *PLoS One*, 2014, **9**, e110709.
14 G. You, J. Hou, P. Wang, Y. Xu, C. Wang, L. Miao, B. Lv, Y. Yang and H. Luo, *Environ. Res.*, 2016, **151**, 698–705.
15 N. Tripathy, T. K. Hong, K. T. Ha, H. S. Jeong and Y. B. Hahn, *J. Hazard. Mater.*, 2014, **270**, 110–117.
16 M. A. Wells, A. Abid, I. M. Kennedy and A. I. Barakat, *Nanotoxicology*, 2012, **6**, 837–846.
17 J. M. Pettibone, D. M. Cwiertny, M. Scherer and V. H. Grassian, *Langmuir*, 2008, **24**, 6659–6667.
18 A. Philippe and G. E. Schaumann, *Environ. Sci. Technol.*, 2014, **48**, 8946–8962.
19 K. A. Huynh and K. L. Chen, *Environ. Sci. Technol.*, 2011, **45**, 5564–5571.
20 Y. Zhang, Y. Chen, P. Westerhoff and J. Crittenden, *Water Res.*, 2009, **43**, 4249–4257.
21 S. K. Fanourakis, J. Peña-Bahamonde, P. C. Bandara and D. F. Rodrigues, *npj Clean Water*, 2020, **3**, 1.
22 A. R. Petosa, D. P. Jaisi, I. R. Quevedo, M. Elimelech and N. Tufenkji, *Environ. Sci. Technol.*, 2010, **44**, 6532–6549.
23 I. K. Konstantinou and T. A. Albanis, *Appl. Catal. B Environ.*, 2004, **49**, 1–14.
24 Y. Pang, Z. Tong, L. Tang, Y. Liu and K. Luo, *Open Chem.*, 2018, **16**, 401–406.
25 D. F. Rodrigues and M. Elimelech, *Biofouling*, 2009, **25**, 401–411.
26 K. M. Buettner, C. I. Rinciog and S. E. Mylon, *Colloids Surfaces A Physicochem. Eng. Asp.*, 2010, **366**, 74–79.

27 J. Liu, C. Dai and Y. Hu, *Environ. Res.*, 2018, **161**, 49–60.

28 V. A. Petrochenkov, I. G. Gorichev, V. V. Batrakov, A. D. Izotov and A. M. Kutepov, *Theor. Found. Chem. Eng.*, 2004, **38**, 386–393.

29 M. N. Hull, *J. Electroanal. Chem.*, 1972, **38**, 143–157.

30 A. R. Head, C. Gattinoni, L. Trotochaud, Y. Yu, O. Karslıoğlu, S. Pletincx, B. Eichhorn and H. Bluhm, *J. Phys. Chem. C*, 2019, **123**, 16836–16842.

31 Y. H. Peng, C. ping Tso, Y. chun Tsai, C. ming Zhuang and Y. hsin Shih, *Sci. Total Environ.*, 2015, **530–531**, 183–190.

32 and S. K. Kontogeorgis, Georgios M., *Introduction to Applied Colloid and Surface Chemistry*, John Wiley & Sons, Ltd, 2016th edn.

33 S. K. Misra, A. Dybowska, D. Berhanu, S. N. Luoma and E. Valsami-Jones, *Sci. Total Environ.*, 2012, **438**, 225–232.

34 J. Schott, O. S. Pokrovsky and E. H. Oelkers, *Rev. Mineral. Geochemistry*, 2009, **70**, 207–258.

35 X. Gao, Q. Guo, G. Tang, W. Peng, Y. Luo and D. He, *J. Water Reuse Desalin.*, 2019, **9**, 301–309.

36 B. Zhou, X. Zhao, H. Liu, J. Qu and C. P. Huang, *Appl. Catal. B Environ.*, 2010, **99**, 214–221.